



iJRASET

International Journal For Research in
Applied Science and Engineering Technology



INTERNATIONAL JOURNAL FOR RESEARCH

IN APPLIED SCIENCE & ENGINEERING TECHNOLOGY

Volume: 6 Issue: IV Month of publication: April 2018

DOI: <http://doi.org/10.22214/ijraset.2018.4804>

www.ijraset.com

Call:  08813907089

E-mail ID: ijraset@gmail.com

Interactive Growcut Multi-Label N-D Segmentation Based Algorithm for SCLERA Segmentation

Laarni R. Hellwig¹, Gerald Cayabyab², Ma. Cristina Aragon³, Ruji P. Medina⁴

^{1, 2, 3, 4}Graduate Studies, Technological Institute of the Philippines

Abstract: This paper presents a computationally efficient sclera detection, segmentation and enhancement approach. The proposed sclera detection and segmentation approach is developed based on the cellular automaton which evolves using the Grow-Cut algorithm and enhancement approach based on Multiscale Retinex. The major advantage of the developed approach is its computational simplicity, speed and accuracy as compared to the prior detection, segmentation and enhancement approaches developed for sclera segmentation images. The new used approach was tested in Intel i5 4570 with 3.2 GHZ processor and 16GB RAM and Intel Dual Core with 2.48GHZ processor and with 2GB RAM. Using these two different units, the result shows that segmentation under Intel i5 segment sclera for three 3 hours with an image size of 640x480 pixels while in Intel Dual Core 2GB RAM having the same image size segments the sclera for fourteen (14) hours and eighteen (18) minutes. The experimental results obtained from ND-IRIS 0405 database and publicly available images and respectively achieved better performance in terms of computational simplicity, speed and accuracy as compared to the previous proposed method. Multiscale Retinex enhanced image very fast with a highest minimum execution time of seventeen seconds (17secs) for an image size of 640 x 480 pixels for both colour and gray scale. The proposed approach for enhancement shows better performance in enhancing low contrast, dark with poor illumination images but colour rendition is quite poor for images having good illumination. The experimental results presented in this paper clearly demonstrate the applicability of the proposed sclera detection, segmentation and enhancement approach, i.e., significant reduction in computational complexity in detection segmentation and enhancement while providing comparable segmentation and enhancement performance.

Keywords: Sclera, Growcut, Multiscale Retinex, Cellular Automaton, Interactive Image Segmentation

I. INTRODUCTION

Our eyesight is one of the most precious senses that serve as the unique window to our health but it's easy to take the gift of sight for granted until it starts to fail. The sclera region (the white outer coat of the eye) comprises a unique and stable blood vessel structure which can be analysed to identify humans [1]. Sclera is shown to be of significant importance for eye and iris biometrics. [2].

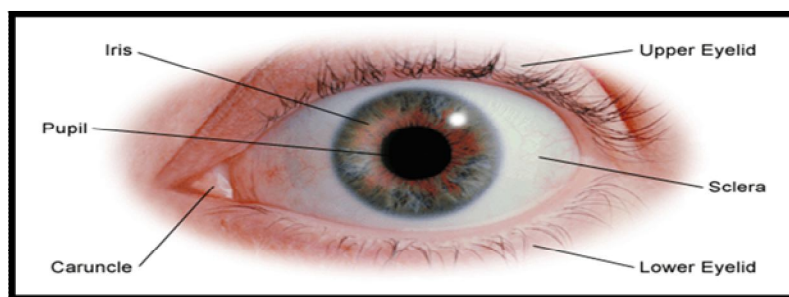


Fig 1. Anatomy of the eye

According to the article written by Rory Jean Jacques for countless millennia, we humans have peered into each other's eyes to see our response or reaction to our environment—and to determine our relative health. Written records from a thousand years ago show that the Chinese used sclera markings to help them understand patient health conditions—over against what they learned from acupuncture pulses. Native American cultures, including the Blackfoot and the Nez Perce tribes, are known to have used sclera markings to discern maladies. There are many maps on the body: the skin, the hands and feet, the nails, the pulses, and so

on. Physicians depend on the eyes—an easily visible natural body map—to provide vital health data. As a direct extension of the brain, the eyes are a very direct representation of bodily conditions via the nervous system. The scleras connect immediately to the brain's dura mater. Theoretically, other systems also express data via the scleras: the endocrine, lymphatic and cardiovascular systems seem to be showing us data thru sclera markings. [3]

The sclera segmentation accuracy has some drawbacks and many researchers continuous to present different algorithms to mitigate those problems. From manual to semi-automated and lastly, it comes to fully automated. Previously study is manual based segmentation, it has been applied by [4] and [5] the study is an unreliable approach for real-time applications because of the human supervision required with the segmentation process and the expensive processing time. In the semi- automated method suggested by [6], [7] and [8] based on K-means clustering, the eyelids included in the resulting sclera image were manually corrected. After that, two automated strategies were suggested based on sclera pixel thresholding and a sclera shape contour to extract sclera regions. [9] used the HSV color space with histogram equalization [10] used the same and low-pass filtering [7] in order to extract the sclera. For grayscale images, Otsu's thresholding method was applied by [11], [12], [13], [14], [15] to detect sclera regions as the intensity of the sclera area is different from the background. Among those algorithms presented by different researchers were thresholding, clustering (k-means), histogram based segmentation in combination with feature enhancement method came out the most used algorithm.

The implicit segmentation method used by different researchers mentioned above, shows degree of performances. But employing efficient and correct segmentation process is a difficult task. According to the work presented by Crihalmeanu, when thresholding and clustering methods (K-Means) is used for segmentation, the final solution depends largely on the initial set of clusters. It shows that the algorithm is fast but it does not guarantee a good sclera-eyelid contour detection. Another one, the K-means algorithm erroneously labels portion of the sclera as being the iris (mainly the corners of the sclera that are less illuminated and have lower intensity values). The algorithm is failed to segment the sclera region properly for a total number of 151 images and due to improper illumination and plenty of mascara found on the image. Another method is Histogram – based segmentation method which can segment also fast it take one pass to read the intensity value of the pixels and to create the histogram but there is a difficulty in identifying which peaks and valleys (the boundaries between the region of interest are significant. The four clusters often overlap meaning they are undistinguishable. Likewise, the boundaries between regions that are to be segmented are characterized by changes in the intensity values of pixels which are known as edges. Unfortunately, these methods results in a multitude of disconnected segments from which it is difficult to select the proper boundaries of the sclera region. The region growing and split and merge method were also employed without satisfactory results due to the large variation and intensity values across the sclera region [16].

Further, due to improper illumination, high frequency or blend images, overlapping of region of interest, segmentation based on sclera region are less robust and do not provide good results. Therefore, alternative methods that overcome the problem of intensity variations have to be used.

II. RELATED LITERATURE

Segmentation is considered as an important step in image processing and computer vision applications, which divides an input image into various non-overlapping homogenous regions and helps to interpret the image more conveniently [17].

Sclera images provide information on the changes in sclera vascular structure, which are common in diseases such as diabetes. [8] proposed the technique of detecting diabetic from sclera using k-means clustering thresholding, occlusion, glaucoma, hypertension, cardiovascular disease and stroke [18]. According to Nguyen, Bhuiyan, Park, & Ramamohanarao, the early exposure of these changes is important for taking preventive measure and hence, the major vision loss can be prevented [19]. [20] proposed the method for detection of diseases on sclera using sobel filter and separating the left half and right half of the eye based on iris boundary. [21] proposed the method for blood vessel detection in sclera using frangi filter and wavelet transform. They detected the sclera area based on Otsu's thresholding method.

In sclera segmentation process, researchers proposed different algorithms to segment, enhance and extract the sclera properly. [22], proposed the sclera segmentation using binary conversion and edge detection by edge detection operator sobel with popup menu and from binary image, edge is detected with edge detecting operators like sobel, canny, prewitt and log. [10] proposed the sclera based biometric recognition using histogram equalization for feature enhancement, line descriptor, sobel and Otsu's thresholding for feature extraction. [23] introduced a sclera recognition and validation where sclera segmentation was performed by Fuzzy logic – based clustering and fuzzy logic based brightness preserving dynamic fuzzy histogram equalization to enhance vessel pattern. S & Senthamilarasu used a clustering algorithm to classify the colour eye images into three clusters - sclera, iris, and background, and

Otsu's thresholding based method for grayscale images, and used a bank of multi directional Gabor filters for vascular pattern enhancement. And contrast limited adaptive histogram equalization (CLAHE) to enhance the green colour plane of the RGB image, and a multi-scale region growing approach to identify the sclera veins from the image background [24]. [25] used automated sclera segmentation with Gabor filter and Histograms of Oriented Gradients for image normalization. [26] proposed a novel sclera segmentation based on machine learning techniques that operates at pixel-level. The proposed approach employs three feature types: statistical image features, Zernike Moments and Histogram of Gradients (HoG)-like features [27], automated sclera segmentation system with occluded eye detection and Gabor wavelet filter and kernel function for smoothing [28], Fuzzy Clustering Means (FCM) based segmentation has been proposed, Fuzzy logic-based Brightness Preserving Dynamic Fuzzy Histogram Equalization (BPDHE) is used to enhance the sclera vessel patterns. The work from [23] performed by Fuzzy Cmeans clustering to segment sclera and Fuzzy logic-based Brightness Preserving Dynamic Fuzzy Histogram Equalization (BPDHE) with Discrete Meyer to enhance the sclera vessel patterns.

With all the different algorithms used for sclera segmentation, GrowCut Interactive Multi-Label N-D Image Segmentation Algorithm was not used. GrowCut algorithm is a new used algorithm to be used for segmenting the sclera. GrowCut algorithm introduced by [29], is capable of solving moderately hard segmentation tasks; easy in implementing and allows efficient parallel implementation; works with images of any dimension $N \geq 1$; performs multi-label image segmentation; is extensible, allows constructing new families of segmentation algorithms with specific properties; and is truly interactive - the user observes the process of computing the segmentation and is able to make modifications and corrections at any time. Grow Cut has been used by researchers like [30], [31] and [32] in segmenting medical images in combination with different feature extraction algorithm.

GrowCut interactive multi-label N-D Image Segmentation has been also compared with graph cuts [33], Graph Cut [34] and Intelligent Scissors [35] with several powerful techniques for interactive image segmentation. They seem to significantly outperform earlier methods both by resulting segmentation quality and required user effort [29]. The GrowCut algorithm is a widely used interactive tool for segmentation because of several key features: 1) natural handling of N-D images, 2) support of multi-label segmentation, 3) on-the-fly incorporation of user input, and 4) easy implementation. [31]

A new technique for the enhancement of colour image using Multiscale Retinex was proposed to enhance the sclera region. It has been used before in contrast enhancement of spinal cord medical images [36]. According to the study of [37], Retinex is the advance technique for the color image enhancement because it is based on color constancy theory and provide dynamic range compression and preserve most of the detail of an image. Modern techniques Retinex (SSR & MSR) performs much better than those gamma correction, contrast stretching, histogram equalization enhancement techniques because it is based on the colour constancy theory.

The purpose of image enhancement is to get finer details of an image and highlight the useful information. During poor illumination conditions, the images appear darker or with low contrast. Such low contrast images needs to be enhanced. In the literature many image enhancement techniques such as histogram equalization [10], and Contrast-limited adaptive histogram equalization (CLAHE) [38], [24] and [39] has been used.

III. DESIGN ARCHITECTURE

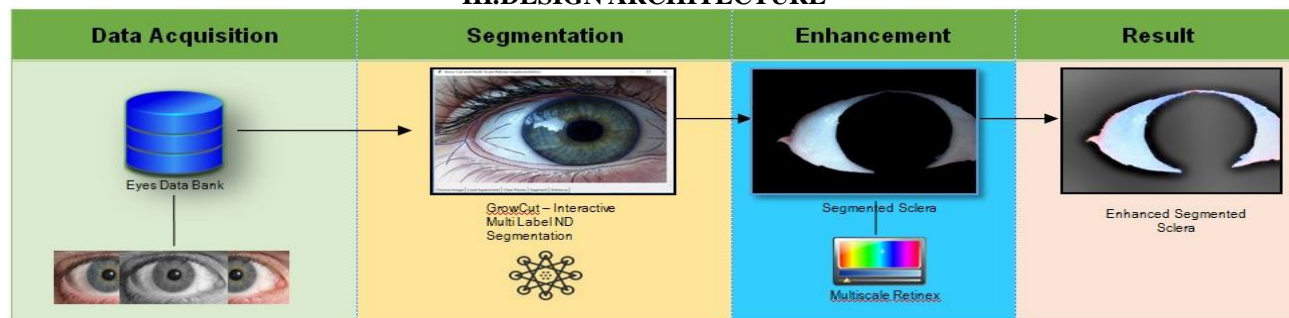


Fig. 2. Design Architecture

The process went through three major processes: Data Acquisition, Segmentation and Enhancement.

A. Data Acquisition

In Data acquisition, a license agreement has been downloaded to be signed by the authorized signatory for research and sent by the research institution to the University of Notre Dame du Lac requesting to use their images known as ND-IRIS-0405 Database [40] for the proposed study. Upon approval, the data will be collected from their image repository.

B. Sclera Segmentation

Interactive GrowCut algorithm [29] with Cellular automata (CA) were introduced by Ulam and von Neumann [41] and employed to segment the sclera region. When user starts the segmentation by specifying the segmentation seeds, the seeded cells labels are set accordingly, while their strength is set to the seed strength value. This sets the initial state of the cellular automaton. GrowCut algorithm requires initialization of seed points which provides the initial labels to indicate the foreground (+1) and background (-1) (sclera and non- sclera) pixels.

In order to facilitate such process, the following rules were employed:

$$l_k = \begin{cases} +1 & \text{if } g_k < \text{mod}(I) - \varphi_f \sigma(\tilde{I}), \\ -1 & \text{if } g_k > \text{mod}(I) + \varphi_b \sigma(\tilde{I}), \\ 0 & \text{Otherwise,} \end{cases}$$

where g_k denotes the intensity value at pixels k, $\text{mod}(I)$ and $\sigma(\tilde{I})$ corresponds to the mode and the standard deviation of the image \tilde{I} [42] At each discrete time $t + 1$, the pixel x may be experiencing a state transition based on the cost function, as defines as follows:

$$\lambda(x, y, \xi_y(t); y \in N(x)) = \left(1 - \frac{\|g_x - g_y\|_2}{\max \|g\|_2} \right)^{-1} \cdot \xi_y(t)$$

The $(.)^{-1}$, $N(x)$ and $\xi_y(t)$ are respective denote the monotonous decreasing function, the neighborhood pixels of x and the energy of pixel y at time t. The image pixel which represents a higher cost λ is attempting to spread its influence to the neighborhood pixels. The rules of bacteria growth and competition are obvious - at each discrete time step, each cell tries to ‘attack’ its neighbors. The following are the steps on how the sclera segmentation takes place. [42]

C. Sclera Image Enhancement

Enhancement can be applied once the vessel structure seen in the sclera region is difficult to recognize in order to reduce the low contrast, dark portion of the image and having poor illumination conditions. The purpose of image enhancement is to get finer details of an image and highlight the useful information because there were images that appear darker or with low contrast. Such low contrast images needs to be enhanced. Multiscale Retinex will be applied to enhance the sclera vessel to reduce various lighting conditions. This method provides balance between contrast and luminance

D. GrowCut – Interactive Multi-Label ND Segmentation Algorithm

According to Li, Xiaoqiang, Chen, Jingsong & Fan, Huaifu one of the main advantages of interactive segmentation algorithm is that it provides a globally or locally optimal solution for image segmentation when the cost function is clearly defined. Energy minimization is made use of within most recently proposed segmentation frameworks Interactive segmentation has been becoming more and more popular to alleviate the problems inherent to fully automatic segmentation which seems to never be perfect [30].

GrowCut is an interactive multi-label segmentation of N-dimensional images, given a small number of user-labelled pixels, where the rest of the image segmented automatically by a Cellular Automaton. The process is iterative, as the automaton labels the image, user can observe the segmentation evolution and guide the algorithm with human input where the segmentation is difficult to compute. In the areas, where the segmentation is reliably computed automatically no additional user effort is required [29].

A cellular automaton is generally an algorithm were introduced by Ulam and von Neumann [41] they been used it to model a wide variety of dynamical systems in various application domains, which includes denoising images and edge detection [42]. CA discrete in both space and time, that operates on a lattice of sites $p \in P \subseteq \mathbb{Z}^n$ (pixels or voxels in image processing). A (bi-directional, deterministic) cellular automaton is a triplet $A = (S, N, \delta)$, where S is an non-empty state set, N is the neighborhood system, and $\delta : SN \rightarrow S$ is the local transition function (rule). This function defines the rule of calculating the cell’s state at t +1 time step,

given the states of the neighborhood cells at previous time step t . Commonly used neighborhood systems N are the von Neumann and Moore neighborhoods:

1) von Neumann neighborhood

$$N(p) = \{q \in Z^n : \|p - q\|_1 := \sum_{i=1}^n |P_i - q_i| = 1\};$$

2) Moore neighborhood

$$N(p) = \{q \in Z^n : \|p - q\|_\infty := \max_{i=1..n} |P_i - q_i| = 1\};$$

The cell state S_p in our case is actually a triplet $(l_p, \theta_p, \vec{c}_p)$ - the label l_p of the current cell, 'strength' of the current cell θ_p , and cell feature vector \vec{c}_p , defined by the image. Without loss of generality we will assume $\theta_p \in [0,1]$.

A digital image is a two-dimensional array of $k \times m$ pixels. An unlabelled image may be then considered as a particular configuration state of a cellular automaton, where cellular space P is defined by the $k \times m$ array set by the image, and initial states for $\forall p \in P$ are set to:

$$l_p = 0, \theta_p = 0, \vec{c}_p = RGB_{p_i}$$

where RGB_{p_i} is the three dimensional vector of pixel's p color in RGB space. The final goal of the segmentation is to assign each pixel one of the K possible labels. The initial, incomplete user-labelling is often sufficient to allow the entire segmentation to be completed automatically, but by no means always. User can add additional gesture in the form of brushing pixels for adding new segmentation constraints [29].

E. Experimental Results and Evaluation

Python Interpreter and ND-IRIS-0405 Database [40] will be used to evaluate the proposed segmentation method based on their applicability, computational simplicity and accuracy. The sclera segmentation will be evaluated against the previously proposed algorithm if the accuracy will vary from the previous record by presenting the results of the previously conducted study.

1) Sclera Segmentation Results

The following figures show how GrowCut algorithm segments the sclera through user interaction and cellular automaton. These images were experimented on Intel i5 and Intel Dual Core showing more user interaction by selecting points and labels for segmentation.

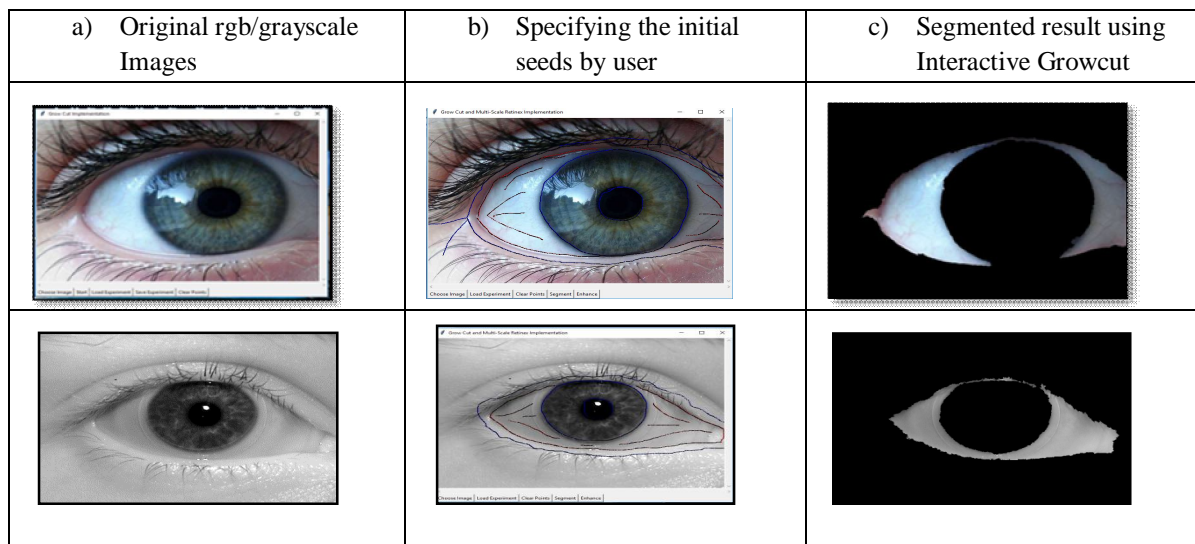


Fig. 3. Segmentation of rgd and grayscale image. (a) Source image, (b) user-specified seeds, (c) segmentation result

The algorithm has been experimented using different eye images. Out of 356 folders that composed of 64,981 image files from ND-IRIS-0405 [40] dataset, only three (3) images were randomly selected and used for the experiment and the rest of the image was use as a training data set. Another seventeen (17) publicly available images in different sizes were also used for the study. The aim of the study is to test the applicability, speed and accuracy of the algorithm in different sizes wherein the dataset from ND-IRIS-0405 [40] compose of images having the same sizes. The result of the segmentation varies in different ways. It was noticed that user interaction has a great impact in the result of the segmentation. As shown in Fig. 3, the result shows that segmented sclera shows edge smoothness and accurately segmented. While in Fig. 4, the result shows that most of the segmented sclera includes other portion of the eye outside the sclera region after segmentation. Thus, user interaction is very important in doing hard segmentation task. The less amount exerted in specifying initial seeds affect much in the accuracy of the segmentation. Upon analysing the image, starting from the selection of labels or points and based on the result of the segmentation, it was found out that selection of labels through brushing, the distance of selected points also affects on the segmentation result as shown in Fig. 4 and 7.

Fig. 4, shows segmented images showing less amount exerted by the user, this is done through brushing using the mouse. The segmentation results show parts of the eye was included in the segmentation.


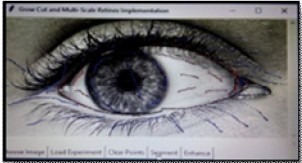
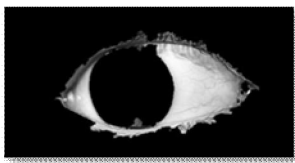
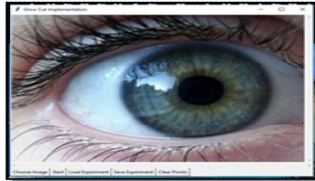

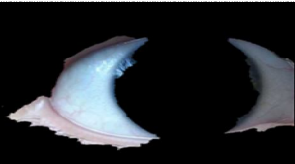

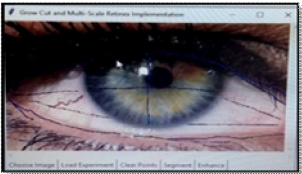
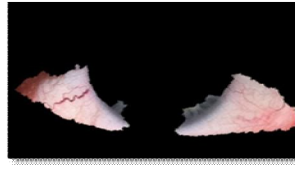
Original rgb/grayscale Images	Specifying the initial seeds by user	Segmented result using Interactive Growcut
		
		
		

Fig. 4 Segmented sclera with less effort exerted

It was observed that after providing the result and the user were not satisfied for the result acquired (see Fig. 4), adding additional gestures is possible. To achieve smoother boundary, an extension to the automata local transition rule is modeled with two additional conditions. First: the cell, that has too many enemies around $enemies^t(p) \geq T_1$ is prohibited to attack its neighbors. Second: the cell that has $enemies^t(p) \geq T_2$ is forced to be occupied by the weakest of it's enemies, no matter the cell's strength. The segmented image can be reloaded and the user can start to add additional gesture in the image as illustrated in Fig. 5 to get an accurate segmentation result. The enemies' number is defined by:

$$enemies^t(p) = \max_{l=1, K} \left(\sum_{q \in N(p), \substack{l_t = l \\ q \neq p}} 1 \right)$$

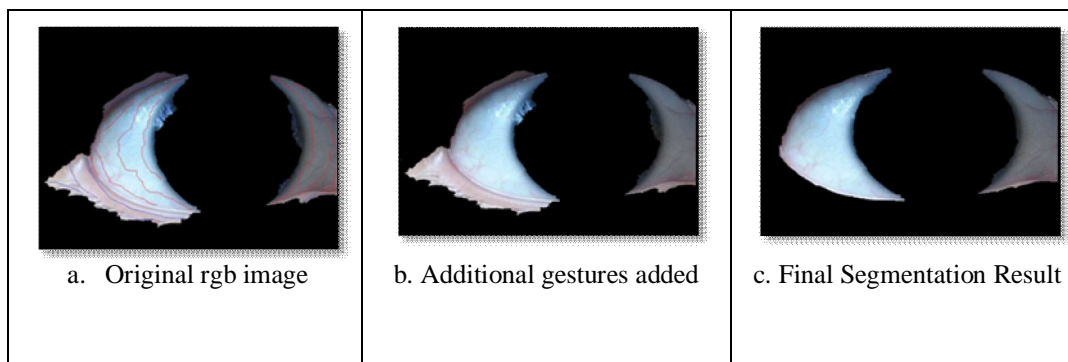


Fig.5 Adding gestures to the segmented image

a) Sclera Segmentation accuracy

To evaluate the accuracy of the proposed algorithm based on sclera detection and segmentation versus with the most common used algorithm like Kmeans the result was compared from the previous study conducted. The researcher was not being able to test the method by itself but by presenting the previous study [16] conducted. The previous study shows that employing K-means algorithm in sclera segmentation, shows even promising performance but it was found out that it erroneously labels portion of the sclera as being the iris while on the other hand applying interactive GrowCut shows better performance by providing the result presented by previous research and the current result of the experiment as shown in the figure below.

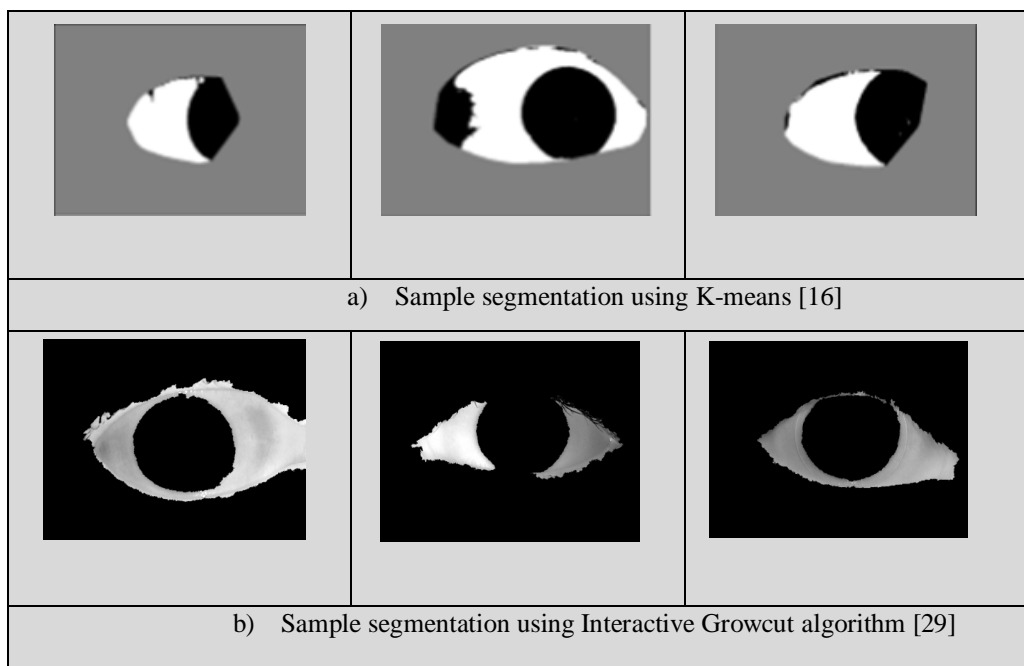


Fig. 6. K-means and Growcut segmentation accuracy.a) Sample segmentation using K-means b) Interactive Growcut algorithm

The smoothness of the segmented images and the results of the segmentation accuracy definitely depend on the user amount of effort exerted in initially specifying seeds or labels. As shown in Fig. 7 those encircled with red, shows the distance of the initial labels that affect on the accuracy of the segmentation. Once the attackers force is greater or stronger (blue) than the defender's strength (red) the defending cell is conquered and it will occupy over the image as an example show in Fig. 7.

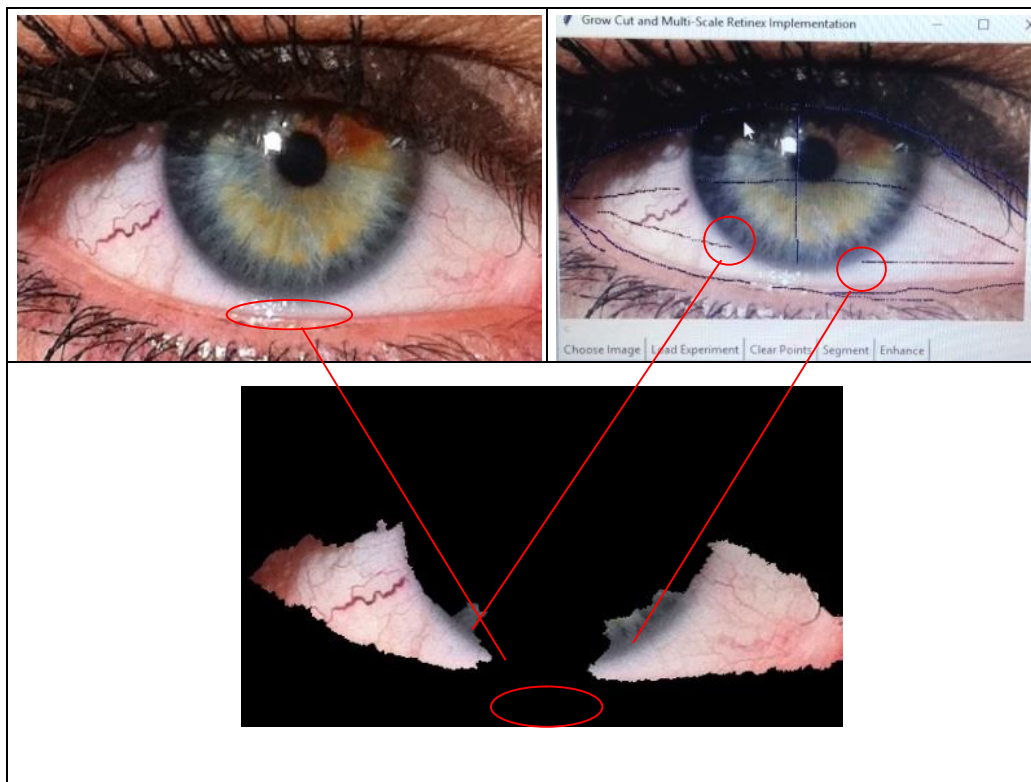


Fig. 7. Sample 1- Image Analysis based on initial selection of labels

The image in Fig. 8 shows another example of segmentation where defenders is stronger than the attackers. Based on the segmentation results, attackers (blue) were not strong enough to attack neighbours that the defenders (red) include portion of the eyelashes and eyelid on the segmented sclera region. Thus, the distance in selecting labels it's either the attackers or defenders will provide different result based on the initial value that has been selected by the user.

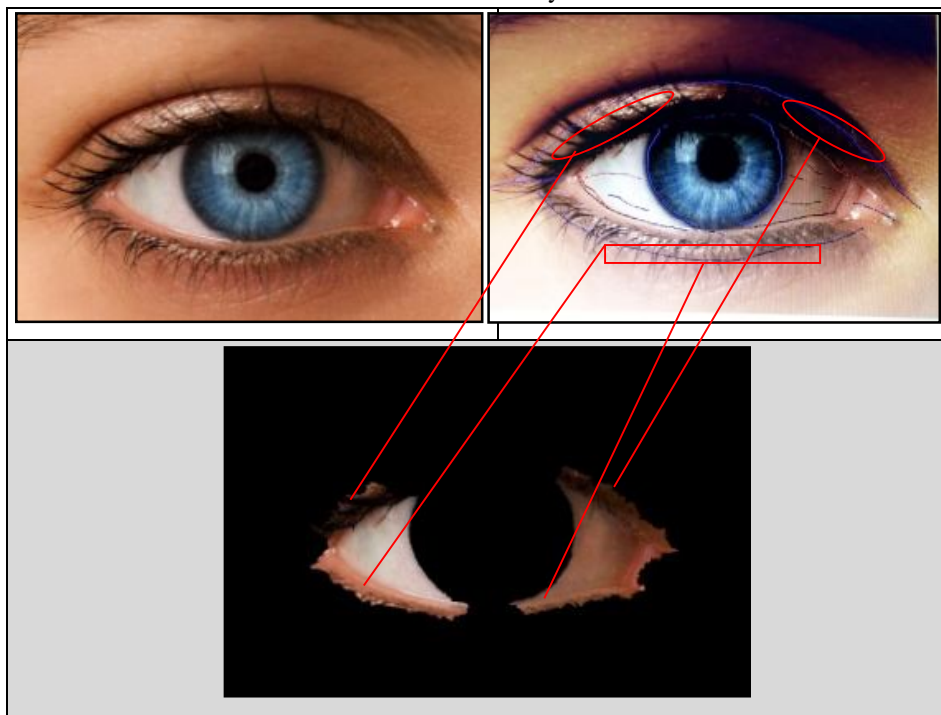


Fig. 8 Sample 2- Image Analysis based on initial selection of labels

b) Speed and algorithmic applicability

Speed is very important in a certain study. The concerned of this study is not only how fast the new applied approach in segmenting the sclera but how fast the recomputation takes place once the user adds more seeds to treat and display a certain result without compromising the speed and accuracy and user convenience. The researcher observed that during segmentation takes place the computation time does not depend only on the number of labels selected but depends on the specification of the computer hardware where the algorithm was implemented. It was also observed that larger image needs longer time to display the result, segmentation speed was also affected by the size of the image, type and format. However, the segmentation accuracy depends on the user interaction by initially selecting and specifying the seeds to be segmented wherein the rest of the segmentation is done by Cellular Automaton.





The results of time execution tested in two different computer units with different sizes of eye images are shown in Table 2. Time is calculated per seconds using Python software as described below:

```

time_recorded.append(time.time())
output_image = growcut(filename,label,strength)
plt.imsave(output_image_file,output_image)
time_recorded.append(time.time())
with open(output_image_file+"_test_time.txt",'w+') as
output_text_time_file:
output_text_time_file.write("start_interaction")
output_text_time_file.write(str(recorded_time[0]))
output_text_time_file.write("end_interaction_start_segmentation")
output_text_time_file.write(str(recorded_time[1]))
output_text_time_file.write("end segmentation")
output_text_time_file.write(str(recorded_time[2]))
output_text_time_file.write("interaction_time")
output_text_time_file.write(str(recorded_time[1]-recorded_time[0]))
output_text_time_file.write("segmentation_time")
output_text_time_file.write(str(recorded_time[2]- recorded_time[1]))

```

TABLE I
RESULTS OF THE EXECUTION TIME OF DIFFERENT IMAGE SEGMENTED
Intel i5 4570 – 3.20 GHz- 16GB VS.
Intel Dual Core N3060c- 2.48GHz- 2G

Original image	Size pixels	Segmentation	Execution Time				
			Intel i5 4570 – 3.20 GHz- 16GB		Intel Dual Core N3060c- 2.48GHz- 2GB		Time variation
	640 x 480		9348.21s	3hrs	49614.32	14.18hrs	
	320 x 240		2339.68s	39mins	12364.68	3.43hrs	3.04hrs



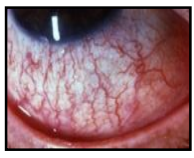

	320 x 240		2284.58s	38mins	12262.54	3.41hrs	3.03hrs
	252 x 186		1418.30s	23mins	7645.52	2.12hrs	1.25hrs

Table 1 shows the time variations of two different computer units and four rgb image in different pixels were used for the experiment. It was observed that an image having the size of 640px x 480px segmented in Intel i5 – 3.2GHz with 16GB RAM is faster compared to the segmentation done using Intel Dual Core N3060- 2.48GHZ in 2GB RAM with a time variation of eleven (11) hours and eighteen (18) minutes . Next image having a size of 320px x 240px was segmented using Intel i5, displayed results after thirty nine (39) minutes while in Intel Dual Core displayed results after three (3) hours and forty three (43) minutes with a time variation of three (3) hours and four (4) minutes. Another image segmented was the image that reloaded for additional gesture. It was found out that the speed and time variation doesn't depend on the selection of labels on the image but on the actual process of the segmentation. As we observed the original image and the image segmented with the same size got only one (1) minute time variation using Intel i5 from the original image versus segmented image with additional gesture added. Another segmentation was also tested using the Intel Dual Core that produced results which is very close to each other same with the variation time of three (3) hours and four (4) minutes from original image and three(3) hours and three (3) minutes from the segmented image with additional gesture added. Next, having the size of 252px x 186px the image was implemented in Intel i5 that display result after twenty three (23) minutes while in Intel Dual Core results display after two (2) hours and twelve (12) minutes. The time variations of two different units are one (1) hour and twenty five (25) minutes. Thus, a time variation does not depend on the labels selected but on the size of the image, type, and format and hardware specification.

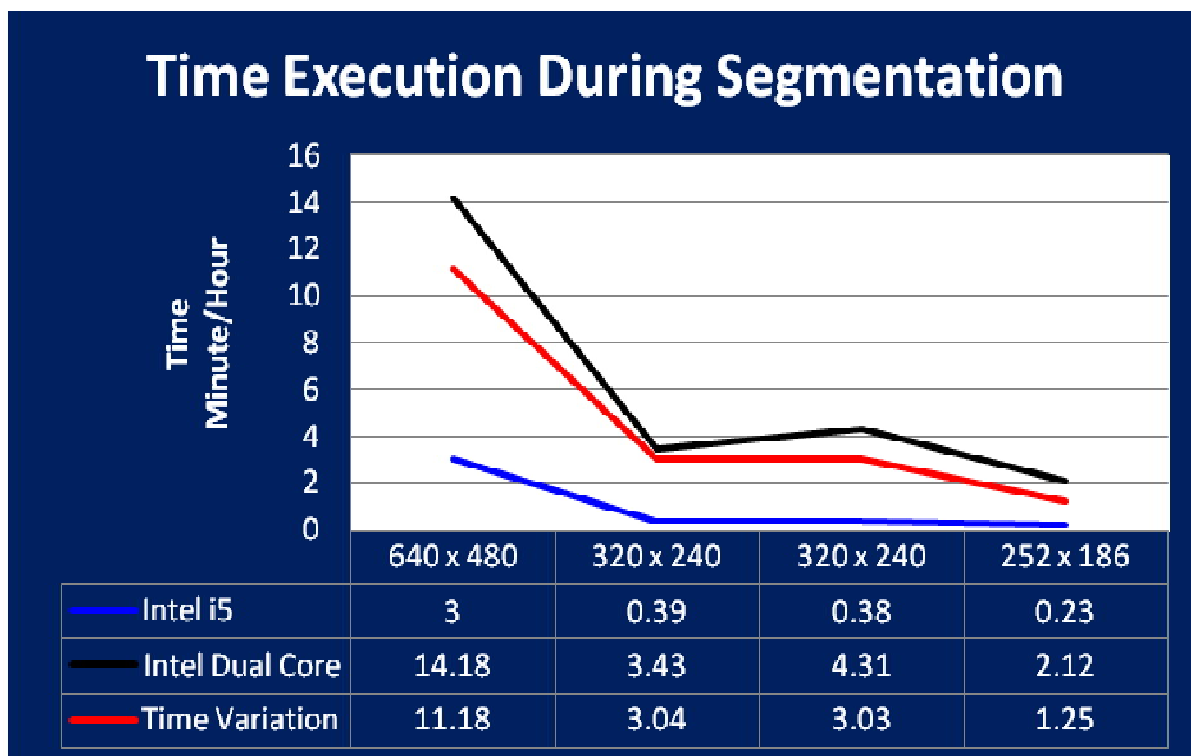
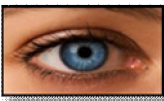
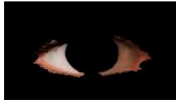

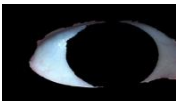
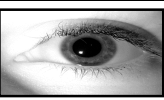
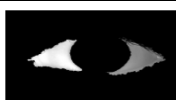
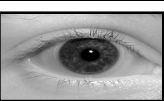

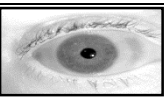


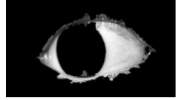
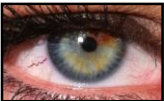


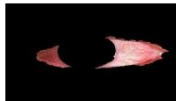




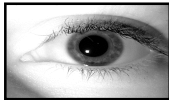

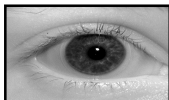

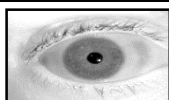

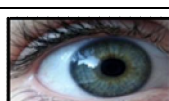
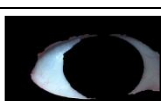
Fig. 9: Line Graph Showing the Time Execution during Segmentation with two different units was done using MS Excel.

TABLE II
RESULTS OF THE EXECUTION TIME OF DIFFERENT IMAGE SEGMENTED
Intel Dual Core N3060c- 2.48GHz- 2GB

Original image	Size Pixels	Segmentation	Execution Time	
			Intel Dual Core N3060c- 2.48GHz- 2GB / Sec	Time/Hours
	660 x 440		47431.48	13.13hrs
	640 x 480		49614.32	14.18hrs
	640 x 480		25661.56	7.13hrs
	640 x 480		25292.35	7.03hrs
	640 x 480		25311.61	7.03hrs
	500 x 248		19661.23	5.46hrs
	466 x 281		23261.90	6.46hrs
	274 x 250		10989.26	3.05hrs
	256 x 180		7285.94	2.02hrs




The result of the experiments using Intel Dual Core as shown in Table 2. The first rgb image was experimented with a total size of 660px x 440px takes almost thirteen (13) hours and thirteen (13) minutes to segment and display the result while the image with 640px x 480px takes fourteen (14) hours and eighteen (18) minutes to segment the sclera while the size of 640px x 480px gray scale format takes almost seven (7) hours and thirteen (13) minutes to segment and another image with the same size finished the segmentation after seven (7) hours and three (3) minutes ; another size of image was experimented with a total size of 500px x 480px finished the segmentation after five (5) hours and forty six (46) minutes , the size of 466px x 281px needs six (6) hours and forty six (46) minutes to segment. An image having the size of 274px x 250px takes three (3) hours and five (5) minutes and finally an image with a size of 256px x 180px needs two (2) hours and two minutes to display the segmentation result. The result presented in Table 2 proved that sizes, type and format of different images vary on the algorithm speed.







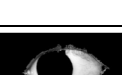


TABLE III
RESULTS OF TESTING ANALYSIS USING INTEL DUAL CORE N3060C- 2.48GHZ- 2GB

Original image	Size Pixels	Segmentation	Execution Time	
			Intel Dual Core N3060c- 2.48GHz- 2GB	Time/Hours
	640 x 480		25661.56	7.13hrs
	640 x 480		25292.35	7.03hrs
	640 x 480		25311.61	7.03hrs
	640 x 480		49614.32	14.18hrs

The results of the segmented sclera presented in Table 3 were analysed based on the colour of the image. As shown in the Table the image having the same pixels size produced different results depends on the colour of the image and format. The three (3) images in gray scale format with a size of 640px x 480px implemented in Intel Dual Core, segmentation result of the two image comes out after seven (7) hours and three (3) minutes and the other one is seven (7) hours and thirteen (13) minutes. The time variation of three images segmented having the same sizes are on the same level and close to each other. Only 10 minutes was the adjacent time of the other image than the other two images. The last image having the same size of pixels from the previous image only in rgb format shows almost half of the total time spent for segmentation process compared from the three images in gray scale format. The 640px x 480px displays the result after fourteen (14) hours and eighteen (18) minutes. The time variation of the image having the same total size is seven (7) hours and five (5) minutes. The result shows that rgb image needs time to compute compared to gray scale image providing the same size of pixel.

TABLE IV
TIME EXECUTION SEGMENTATION SUMMARY

Segmented Sclera	Size	Start Interaction	End Interaction/ Start segmentation	End Segmentation	Interaction Time	Segmentation Time
Intel i5 4570 – 3.20 GHz- 16GB						
	320x 240	1523854212.615104	1523854415.9077318	1523856755.5915542	203.29262781143188	2339.6838223934174
	320x 240	1523869402.9089394	1523869543.715993	1523871828.2916632	140.807053565979	2284.5756702423096
	640x480	1523857896.7828264	1523858086.5556808	1523867434.770368	189.77285432815552	9348.214687347412

	252x186	1523867640. 8951578	1523867753.85 46185	1523869172.155 741	112.9594607 3532104	1418.30112242 69867
Intel Dual Core N3060c- 2.48GHz- 2GB / Sec						
	640x480	1523777680. 0685976	1523777899.84 51693	1523803561.406 6947	219.7765717 5064087	25661.5615253 4485
	640x480	1523807459. 2116277	1523807658.19 21675	1523832950.539 8617	198.9805397 9873657	25292.3476941 58554
	640x480	1523748981. 8429089	1523749212.44 29452	1523774524.053 7572	230.6000363 8267517	25311.6108119 48776
	256x180	1523928399. 0986073	1523928540.07 66551	1523935826.014 2841	140.9780478 477478	7285.93762898 4451
	466x281	1523948985. 097132	1523949150.19 36677	1523972412.097 536	165.0965356 8267822	23261.9038684 36813
	500x248	1523905889. 7646427	1523906099.22 2909	1523925760.455 6434	209.4582662 5823975	19661.2327344 41757
	660x440	1523976393. 2787771	1523976621.73 909	1524024053.220 756	228.4603128 4332275	47431.4816660 88104
	274x250	1523936385. 6250005	1523936651.63 99405	1523947640.895 6056	266.0149400 2342224	10989.2556650 63858

2) Sclera Enhancement Result

Image enhancement after segmentation or before segmentation provides different results. The main purpose of image enhancement is to get finer details of an image and highlight the useful information because there were images that appear darker or with low contrast and poor luminance.

The proposed Multiscale Retinex can be compactly written as

$$F_i(x,y) = \sum_{n=1}^N W_n \{ \log[S_i(x,y)] - \log[S_i(x,y) * M_n(x,y)] \}$$

where the subscripts $i \in R, G, B$ represents the three color bands, N is the number of scales being used, and W_n are the weighing factors for the scales being used, and M_n are the weighing factors for the scales. The $M_n(x,y)$ are surrounded functions given by

$$M_n(x,y) = K_n \exp[-(x^2 + y^2)/\sigma_n^2],$$

where the σ_n are the standard deviations of the Gaussian distribution that determine the scale. The magnitude of the scale determines the type of information that the retinex provides: smaller scales providing more dynamic range compression, and larger scales providing more color constancy. The K_n are selected so that $\iint F(x,y) dx dy = 1$ [43]. Using these formula in the background, the result of enhancement are shown in Table 5 together with time execution.

TABLE V
 ENHANCEMENT RESULT
 Intel Dual Core N3060c- 2.48GHz- 2GB / Sec

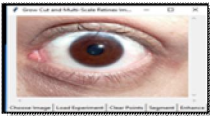









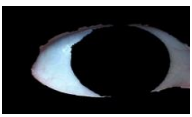

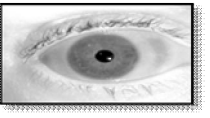
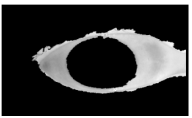

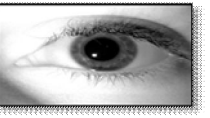
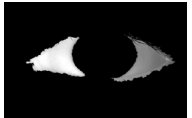

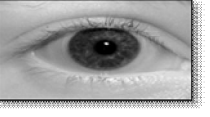


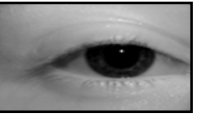


Original Image	Size	Without Enhancement	Result with Retinex Enhancement	Time Execution
	320x240			4.0881290435 79102
	320x240			4.3691403865 81421
	256x180			7.2352311611 17554
	640x480			16.940541744 232178
	640x480			16.851536750 793457
	640x480			16.735560178 756714
	640x480			17.028544664 382935
	110 x 83			0.8080241680 145264

Table 5 shows the result of the experiment done in Intel Dual Core N3060c- 2.48GHz- 2GB using the new proposed Multiscale retinex. The enhancement accuracy was compared based on the segmented image without enhancement and image with enhancement. The results using MultiScale Retinex highlight the colors in most image both bright and dark areas but the noise at the edge of the rgb image was also observed results of poor signal to noise ratio in a certain area of the image.

The result of the experiment shows that an image which is experimented twice through adding additional gesture as shown on the second image having the size of 320px x 240px was enhanced a little bit slower than an image without gesture added with a total time execution of 4.08 seconds. Followed by an image having the size of 256px x 180px enhanced after 7.23 seconds. Next images having the size of 640px x 480px enhanced after 16.94 seconds, 16.85 seconds, 16.73 seconds, and 17.02 seconds. The last image having the size of 110px x 83px was blurry and dark before enhancement. After the image was enhanced it was observed that the

image comes brighter. Based on the experiments, enhancement is possible before and after the segmentation that produced different results depends on the image status. The rgb image which was experimented that show high contrast as shown in Table 5 loses its details after segmentation because of unnatural color rendition during enhancement. The algorithm is fast that can display the enhanced results in seconds. Hence, enhancement can be applied only to those with low contrast dark and poor illumination image to display and highlight useful information as shown on the grayscale image found in Table 5.

The figure below represented in line graph shows enhancement result for both rgb and grayscale images.

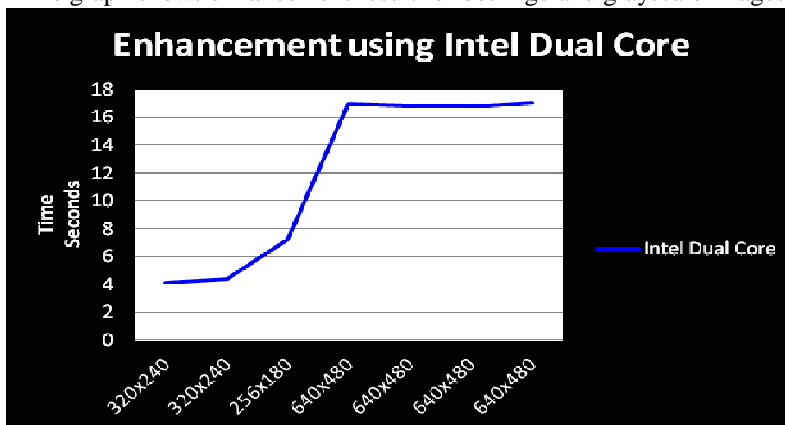


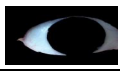
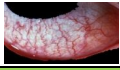


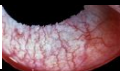





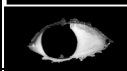




Fig. 10: Line Graph showing the Time Execution during Enhancement

TABLE VI
Enhancement Time Execution Analysis And Summary
Intel Dual Core N3060c- 2.48GHz- 2GB

Segmented Sclera	Size	Start Interaction	End Interaction/ Start Enhancement	End Enhancement	Interaction Time	Enhancement Time
Segmented in Intel i5			Enhanced in Intel Dual Core			
	320x240	1524238199.9 158072	1524238251.3644 538	1524238255.45258 28	51.448646545 410156	4.0881290435791 02
	320x240	1524237969.5 124362	1524238037.2076 027	1524238041.39273 26	67.695166587 82959	4.1851298809051 51
	640x480	1524238359.4 639144	1524238416.9417 498	1524238434.07329 73	57.477835416 79382	17.131547451019 287
	252x186	1524238450.5 908315	1524238491.9741 552	1524238494.48223 5	41.383323669 433594	2.5080797672271 73
Segmented in Intel Dual Core			Enhanced in Intel Dual Core			
	320x240	1524237449.2 557847	1524237479.2107 432	1524237483.57988 36	29.954958438 87329	4.3691403865814 21
	640x480	1524237494.4 16231	1524237528.3423 154	1524237545.28285 72	33.926084518 43262	16.940541744232 178
	252x186	1524237255.4 894948	1524237376.7904 69	1524237380.06857 25	121.30097413 06305	3.2781035900115 967
	640x480	1523713305.3 575878	1523713336.5472 815	1523713353.28284 17	31.189693689 346313	16.735560178756 714
	640x480	1524237601.3 066516	1524237671.9659 126	1524237688.99445 72	70.659260988 23547	17.028544664382 935
	640x480	1524237553.9 781382	1524237576.5508 597	1524237593.40239 64	22.572721481 323242	16.851536750793 457
	256x180	1524237702.3	1524237735.2839	1524237738.03203	32.971057176	2.7480916976928

		128822	394	1	589966	71
	466x281	1524237752.9 965043	1524237785.5295 446	1524237792.76477 58	32.533040285 110474	7.2352311611175 54
	500x248	1524237802.6 00096	1524237839.4052 718	1524237846.54549 84	36.805175781 25	7.1402266025543 21
	660x440	1524237855.2 657762	1524237888.6468 47	1524237905.43038 37	33.381070852 27966	16.783536672592 163
	274x250	1524237915.5 877101	1524237949.0487 797	1524237952.92790 22	33.461069583 89282	3.8791224956512 45

The summarized Table for sclera image enhancement using Multiscale Retinex, shows that images both colour and gray scale enhanced very fast based on the result presented on the table. Based on the experiment, the enhancement time depends also how fast the user interact during the enhancement process. The slower the interaction will give the highest total time of execution.

IV. CONCLUSIONS AND RECOMMENDATIONS

The new used interactive GrowCut algorithm proved the applicability and computational simplicity based on user interactivity and Cellular Automaton in sclera detection and segmentation. The speed and accuracy was being tested and experimented using two computer units – Intel i5 with 16GB RAM and Intel Dual Core with 2GB RAM and it was objectively proved that GrowCut algorithm can segment fast using higher computer specification and accurately segment the sclera region based on user interaction and the rest of the segmentation was done by Cellular Automaton. Thus, the speed also varies based on computer specification, image sizes, type and format. Multiscale Retinex enhanced image very fast and shows better performance in enhancing low contrast, dark and poor illumination images but colour rendition is quite poor for images having good illumination with a highest minimum execution time of sixteen seconds (16secs) for an image size of 640 x 480 pixels both colour and gray scale. Based on the results obtained from the experiments the proposed new used algorithm shows potential sclera detection and segmentation and mitigates the challenges as the previous study presented. It is recommended that more work is needed on how to improve the colour rendition of Multiscale Retinex during enhancement.

V. ACKNOWLEDGMENT

L.R. Hellwig would like to acknowledge the financial support provided by the Commission on Higher Education, K-12 Project Management Unit, Philippines and Romblon State University – San Fernando Campus, San Fernando, Romblon, Philippines.

REFERENCES

- [1] D. Borza, A. S. Darabant & R.. Danescu (2016). Real-time detection and measurement of eye features from color images. Sensors (Switzerland), 16(7). <https://doi.org/10.3390/s16071105>
- [2] R. D. Bharathi, & B. V. Kumar (2017). Automatic Detection of Adenoviral Disease from Eyes Images Using HOG Technique, 1(3), 180–184.
- [3] Rory Jean Jacques – Sclerology - SA's Nature Doc- 0827281658. (2017). Retrieved from <http://www.roryjeanjacques.com/sclerology.html>
- [4] R. Derakhshani, A. Ross, & S. Crihalmeanu (2006). A new biometric modality based on conjunctival vasculature. Artificial Neural Networks in ..., (November), 1–8. Retrieved from http://www.csee.wvu.edu/~ross/pubs/DerakhshaniConjunctiva_ANNIE2006.pdf
- [5] R. Derakhshani & A. Ross, (2007). A Texture-Based Neural Network Classifier for Biometric Identification using Ocular Surface Vasculature. Image (Rochester, N.Y.), (August), 0–5.
- [6] S. Crihalmeanu, A. Ross & R. Derakhshani (2009). Enhancement and registration schemes for matching conjunctival vasculature. Lecture Notes in Computer Science (Including Subseries Lecture Notes in Artificial Intelligence and Lecture Notes in Bioinformatics), 5558 LNCS(June), 1240–1249. https://doi.org/10.1007/978-3-642-01793-3_125
- [7] A. Suganya & M. Sivitha (2015). A new biometric using sclera vein recognition for human identification. In 2014 IEEE International Conference on Computational Intelligence and Computing Research, IEEE ICCIC 2014. <https://doi.org/10.1109/ICCIC.2014.7238324>
- [8] B. N. Latha, M. B. Ushadevi, & Y. Sangeetha (2016). Personal Authentication by Extracting Sclera Veins. International Journal of Advanced Research in Computer and Communication Engineering, 5(6). <https://doi.org/10.17148/IJARCCCE.2016.5696>
- [9] K. Oh, & K. A. Toh (2012). Extracting sclera features for cancelable identity verification. Proceedings - 2012 5th IAPR International Conference on Biometrics, ICB 2012, 245–250. <https://doi.org/10.1109/ICB.2012.6199815>
- [10] S. S. Fargose, A. A. Goregaonkar, & K. C. Khond (2014). A Survey on SCLERA Based Biometric Recognition. The International Journal Of Science & Technoledge, 2321–919. Retrieved from www.theijst.com
- [11] Z. Zhou, E. Du Yingzi, N. L.Thomas, & E. J. Delp (2011). Multi-angle sclera recognition system. IEEE SSCI 2011 - Symposium Series on Computational Intelligence - CIBIM 2011: 2011 IEEE Workshop on Computational Intelligence in Biometrics and Identity Management, 103–108. <https://doi.org/10.1109/CIBIM.2011.5949225>
- [12] Z. Zhou, E. Du Yingzi, N. L.Thomas, & E. J. Delp (2012). A New Human Identification Method: Sclera Recognition. SYSTEMS AND HUMANS, 42(3). <https://doi.org/10.1109/TSMCA.2011.2170416>

- [13] D. Rane, S. Salunke, V. Salunke, M. Choche, B. E.Student, & A. Professor (2015). International Journal of Advanced Research in Computer Science and Software Engineering Use of Biometrics for Authentication -Sclera Recognition, 5(3).
- [14] B. Latha & B. Suma (2015). Image Correction and Feature Extraction for Human Eye. International Journal of Computer Applications, 975–8887.
- [15] K. R. Saranya, S.V. Nivi A N, & J. Thangaraju (2014). Sclera Vein Recognition Using Different Matching Techniques. International Journal For Research In Emerging Science And Technology.
- [16] S. G. Crihalmeanu (2012). Multispectral Scleral Patterns For Ocular Biometric Recognition
- [17] Y. Guo, Y. Akbulut, A. Şengür, R. Xia & F. Smarandache, (2017). An Efficient Image Segmentation Algorithm Using Neutrosophic Graph Cut. Symmetry, 9(9), 185. <https://doi.org/10.3390/sym9090185>
- [18] M. B. Wankhade (2016). Analysis of Disease using Retinal Blood Vessels Detection. International Journal Of Engineering And Computer Science, 5(12), 19644–19647. <https://doi.org/10.18535/ijecs/v5i12.68>
- [19] Y. T. Mahesh, & K. L. Shunmuganathan (2014). Computer Science and Management Studies Human Identification Based on the Pattern of Blood Vessels as Viewed on Sclera Using HOG and Interpolation Technique. International Journal of Advance Research in, 2(9).
- [20] U. T. V Nguyen, A. Bhuiyan, L. A. F. Park & K. Ramamohanarao (2013). An effective retinal blood vessel segmentation method using multi-scale line detection. Pattern Recognition, 46(3), 703–715. <https://doi.org/10.1016/j.patcog.2012.08.009>
- [21] J. S. Anju & S. L. Anju (2014). An Effective Method for Blood Vessel Detection in Sclera, 3(3), 718–722.
- [22] M. M. Sarala, Vijayanand, & M. Malathy (2017). Effective Application for Detection of Diseases from Sclera Image. Int. J. Advanced Networking and Applications, 4(4), 2016–2018.
- [23] A. Das, U. Pal, M. Angel, F. Ballester & M. Blumenstein (2014). Fuzzy Logic Based Sclera Recognition, 561–568.
- [24] S. K. S. & S. Senthilarasu (2015). A Neural Approach for Sclera Vein Recognition. International Journal of Advanced Research in Computer and Communication Engineering, 4(4). <https://doi.org/10.17148/IJARCC.2015.4434>
- [25] S. Suba & S. Babu (2015). International Conference on Futuristic Trends in Computing and Communication (ICFTCC-2015) Human Identification Based on Sclera Vein Recognition Using Histogram of Oriented Gradient. Retrieved from www.internationaljournalsrsg.org
- [26] P. Radu, J. Ferryman & P. Wild (2015). A robust sclera segmentation algorithm. 2015 IEEE 7th International Conference on Biometrics Theory, Applications and Systems, BTAS 2015. <https://doi.org/10.1109/BTAS.2015.7358746>
- [27] R. Parab, (2016). Sclera Pattern Recognition for Identification. International Journal of Computer Applications, 156(7), 975–8887.
- [28] O. G. Hastak (2017). Human Identification Based on Sclera Veins Extraction. International Research Journal of Engineering and Technology, 2395–56.
- [29] V. Vezhnevets & V. Konouchine (2005). GrowCut - Interactive Multi-Label N-D Image Segmentation By Cellular Automata. Graphicon, 150–156. <https://doi.org/10.1016/j.ajodo.2004.07.036>
- [30] X. Li, J. Chen, & H. Fan (2012). Based on Grow Cut of Two Scale Graphs, 90–91.
- [31] Zhu, L., Kolesov, I., Gao, Y., Kikinis, R., & Tannenbaum, A. (2014). An Effective Interactive Medical Image Segmentation Method Using Fast GrowCut. International Conference on Medical Image Computing and Computer Assisted Intervention (MICCAI), submitted.
- [32] C. Rajivegandhi, R. Sankineni, S. Khan & V. Sharma (2015). Skin Ulcer Image Segmentation Based On Grow Cut Method, 10(7), 3010–3013.
- [33] Y. Y. Boykov & M.-P. Jolly (2001). Interactive graph cuts for optimal boundary & region segmentation of objects in N-D images. Proceedings Eighth IEEE International Conference on Computer Vision. ICCV 2001, 1(July), 105–112. <https://doi.org/10.1109/ICCV.2001.937505>
- [34] C. Rother & A. Blake (2004). “ GrabCut ” — Interactive Foreground Extraction using Iterated Graph Cuts.
- [35] E. N. Mortensen & W. A. Barrett (1999). Toboggan-Based Intelligent Scissors with a Four Parameter Edge Model.
- [36] S. Setty, N. K. Srinath & M. C. Hanumantharaju (2014). An improved approach for contrast enhancement of spinal cord images based on multiscale retinex algorithm. International Journal of Imaging and Robotics, 13(2), 112–125.
- [37] A. K. Vishwakarma & A. Mishra (2012). Color Image Enhancement Techniques: A Critical Review. Indian Journal of Computer Science and ..., 3(1), 39–45. Retrieved from <http://www.ijcse.com/docs/INDJCSE12-03-01-071.pdf>
- [38] S. S. Rajole & J. V. Shinde (2017). Integrated Approach for Sclera Recognition and Eye Gaze Detection. International Journal of Emerging Research in Management & Technology, 6, 2278–9359.
- [39] S. Alkassar, W. L. Woo, S. S. Dlay & J. A. Chambers, (2016). Enhanced segmentation and complex-sclera features for human recognition with unconstrained visible-wavelength imaging. In 2016 International Conference on Biometrics, ICB 2016. <https://doi.org/10.1109/ICB.2016.7550049>
- [40] P. Jonathon Phillips, W. Todd Scrugs, Alice J. O’Toole, Patrick J. Flynn, Kevin W. Bowyer, Cathy L. Schott, Matthew Sharpe, "FRVT 2006 and ICE 2006 Large - Scale Experimental Results," IEEE Transactions on Pattern Analysis and Machine Intelligence, in press. <http://doi.ieeecomputersociety.org/10.1109/TPAMI.2009.59>
- [41] J. Von Neuman., (1966). Theory of self-reproducing automata. Information Storage and Retrieval. [https://doi.org/10.1016/0020-0271\(69\)90026-6](https://doi.org/10.1016/0020-0271(69)90026-6)
- [42] Tan, C. W., & Kumar, A. (2012). Efficient iris segmentation using Grow-Cut algorithm for remotely acquired iris images. 2012 IEEE 5th International Conference on Biometrics: Theory, Applications and Systems, BTAS 2012, 99–104. <https://doi.org/10.1109/BTAS.2012.6374563>
- [43] A. Popovici & D. Popovici (2002). Cellular Automata in Image Processing, 1–6.
- [44] Rahman, Z., Jobson, D. J., & Woodell, G. A. (n.d.). Multi-scale retinex for color image enhancement. In Proceedings of 3rd IEEE International Conference on Image Processing (Vol. 3, pp. 1003–1006). IEEE. <https://doi.org/10.1109/ICIP.1996.560995>



10.22214/IJRASET



45.98



IMPACT FACTOR:
7.129



IMPACT FACTOR:
7.429



INTERNATIONAL JOURNAL FOR RESEARCH

IN APPLIED SCIENCE & ENGINEERING TECHNOLOGY

Call : 08813907089  (24*7 Support on Whatsapp)